Article

Not peer-reviewed version

Structural and Safety Design of a Low-Cost Electric Three-Wheeler for Dense Urban Traffic Using a Multidisciplinary FEA Approach

Jubayer Ahmed Sajid , Ivan Grgić * , Ashab Farhan Anon , Toymor Wafi Opul , Md. Ridoan Hasan , Mirko Karakašić

Posted Date: 16 March 2026

doi: 10.20944/preprints202603.1246.v1

Keywords: electric three-wheeler; urban mobility; vehicle stability; structural analysis; braking systems; safety design; low-cost design

 doi:10.20944/preprints202603.1246.v1

Article

Structural and Safety Design of a Low-Cost Electric Three-Wheeler for Dense Urban Traffic Using a Multidisciplinary FEA Approach

Jubayer Ahmed Sajid [1], Ivan Grgić [2,*], Ashab Farhan Anon [1], Toymor Wafi Opul [1], Md. Ridoan Hasan [1] and Mirko Karakašić [2]

[1] Aviation and Aerospace University, Faculty of Aerospace Engineering, Old Airport, Tejgaon Dhaka 1215, Bangladesh
[2] Mechanical Engineering Faculty in Slavonski Brod, University of Slavonski Brod, Ulica 108. brigade ZNG 36, 35000 Slavonski Brod, Croatia
* Correspondence: igrgic@unisb.hr

Abstract

This paper presents the structural and safety design of a low-cost electric three-wheeler intended for use in the densely populated urban environment of Dhaka, Bangladesh. The goal of this project was to improve currently available informally manufactured or unregulated motorised vehicles, which often have unsafe structural features, such as a high centre of gravity and inadequate braking systems. The vehicle is designed to accommodate five people (one driver and four passengers), reach a maximum speed of 30 km/h, and be manufactured locally at an estimated cost of 1200–1400 EUR. The vertical centre of gravity was determined to be 0,642 m above ground level, resulting in a static stability factor of 1,09. Structural performance was evaluated using ANSYS Mechanical under combined static loading conditions and a simulated frontal impact at 30 km/h. The redesigned tubular frame reduced maximum upward deflection by 15,6% and increased energy absorption during frontal collision by 37,3% compared to previous designs. Braking performance analysis showed that the vehicle can stop within 10 metres from 25 km/h, while rotor temperatures maintained a 108 °C margin below the fade threshold for brake fade during repeated emergency braking. The results demonstrate that substantial improvements in structural safety and thermal performance can be achieved in low-cost electric three-wheelers using locally available manufacturing resources.

Keywords: electric three-wheeler; urban mobility; vehicle stability; structural analysis; braking systems; safety design; low-cost design

1. Introduction

There is a pressing need for affordable last-mile personal transportation due to the rapid motorisation of South Asian cities, especially Dhaka. In Bangladesh, battery-powered three-wheelers have become an essential low-cost transit option [1]. Three-wheelers manufactured in developing countries do not follow the same regulatory framework or safety standards as those approved in developed economies (i.e., homologated) [2], resulting in numerous safety issues with current designs, such as rollover instability, inadequate braking, poor structural crashworthiness, and thermal management problems that increase the risk of accidents, rollovers, and electrical fires in crowded city environments.

Rollover resistance in three-wheeled vehicles has been extensively studied. Mathematical frameworks developed by Nguyen et al. [3] indicate reduced inherent stability compared to four-wheeled counterparts, where balance depends largely on the relationship between wheel track width

 doi:10.20944/preprints202603.1246.v1

and the vertical position of the centre of mass. In contrast, research by Ketemaw et al. [4] shows that accident frequency decreases when dynamic indicators are combined with control methods tailored for delta-configuration tricycles. Later work by Ataei et al. [5], which incorporates terrain layout into vehicle behaviour, demonstrates that secure performance requires a static stability factor greater than 1,2. Rodríguez-Licea et al. [6] examined tripped rollover events in three-wheeled vehicles, showing that active control systems reduce lateral sliding and partial loss of ground contact. Jin et al. [7] showed that applying a rollover risk threshold during design enables co-optimisation of power consumption and passenger comfort without compromising stability.

When assessing structural crash performance, engineers rely heavily on finite element analysis to estimate how vehicles respond during collisions [8]. Validation by Ayyakkannu et al. [9] confirmed that simulations of roll cage designs closely match real-world tests. Compliance with braking regulations such as FMVSS 135 [10] requires vehicles to meet stopping distance benchmarks linked to deceleration levels of approximately 0,25–0,30 g. Brake thermal behaviour is a critical design consideration. Research by Talati and Jalalifar [11] showed disc temperatures exceeding 200 °C after multiple hard stops, approaching conditions where braking power decreases. Investigations into heat patterns using FEA were supported by Jaenudin et al. [12], whose work showed good agreement between simulated outputs and measured data.

Battery thermal management is essential for electric three-wheelers using lead-acid chemistry. Damodaran et al. [13] defined flow requirements under different driving scenarios and constructed simplified models of thermal dynamics. Peak efficiency and lifespan occur within 20–25 °C, a range highlighted in a vehicle cooling review by Yavuz et al. [14]. Li et al. [15] accurately predicted lead-acid battery temperature rise during discharge using reduced-order thermal-electrochemical models.

Recent studies have shown that combined methods improve vehicle balance. Nguyen et al. [16] developed active stabiliser bars with fuzzy logic control, reducing tilt and load shifts during movement. Chen et al. [17] proposed cooperative differential braking combined with adaptive suspension for triple-axle models, improving lateral stability. Thermal management of electric drivetrain components is equally critical. Du et al. [18] showed that BLDC motors require precise temperature control to prevent insulation degradation. Overheating beyond safe limits during prolonged use causes irreversible damage to insulation, significantly reducing operational lifespan. While advanced cooling methods offer potential advantages, integrating them into budget models presents challenges. High component costs and maintenance difficulties are contributing factors. Limited availability of sensors and actuators in distribution networks within emerging regions further restricts implementation. Although current three-wheelers in Bangladesh prioritise low fabrication costs, they often lack essential structural protections. In contrast, academic research focused on protection typically proposes methods relying on advanced electronics or materials unsuitable for local workshop conditions and financial constraints.

This work presents an integrated structural, thermal, and electrical safety design of a low-cost electric three-wheeler optimised for dense urban conditions in developing markets. A low-mounted battery and tubular space-frame chassis yield an SSF of 1,09 and a CoG height of 0,642 m. Comparative FEA under static loading and 30 km/h frontal impact demonstrates 15,6 % lower peak positive deflection and 37,3 % greater energy absorption relative to the baseline design. Braking analysis confirms a stopping distance below 10 m from 25 km/h, with rotor temperatures maintaining a 108 °C margin below the fade threshold and motor temperatures within NEMA Class F insulation limits. Manufacturing cost is confirmed within 1200–1400 EUR using locally available processes and materials.

2. Vehicle Concept and Design Targets

One driver sits at the front, with space for four passengers in the back. The vehicle is configured for urban commuting and light commercial operation in dense traffic conditions. At peak, it travels no faster than 30 km/h, matching the slow pace of e-rickshaws across Bangladesh, making it well

 doi:10.20944/preprints202603.1246.v1

suited to narrow streets [2]. CAD models established precise size targets, later consolidated as shown in Table 1.

Table 1. Vehicle dimensional specifications.

Parameter	Value (mm)
Overall Length	2888,8
Overall Width	1050
Overall Height	1670
Wheelbase	2300
Rear Track Width	1400
Ground Clearance	155

Regulations concerning balance during motion inform its stability objectives [3,4], while braking performance is based on brake-related standards [10], heat limits for motor components are guided by previous research on electrical system endurance [13,14]. In city driving scenarios, including monsoon climates, safety during overturning, impact resistance, and heat management are prioritised. See Table 2 for the objectives.

Table 2. Performance and safety design targets.

Target	Value	Justification
Static Stability Factor (SSF)	≥1,2	Required for safe lateral stability [3,5]
Maximum CoG height	≤0,65 m	Low CoG reduces rollover propensity [3,6]
Braking distance (from 25 km/h)	<10 m	Equivalent to 0,25 g deceleration [10]
Brake fade temperature margin	≥45°C	Fade threshold 200°C [19]
Motor thermal limit	<155°C	NEMA Class F insulation limit [20]
Battery thermal limit	<45°C	Preserve electrolyte integrity at 35°C ambient [13,14]
Target cost (manufacturing)	1200-1400 EUR	Local manufacturability

Low placement of the battery pack helps reduce the overall height of the centre of gravity. Positioned within the frame, the 136 kg unit supports a balanced weight layout. Structural strength is not compromised despite lightweight goals. At 387 kg, the empty vehicle mass includes all standard components. Designed to carry up to 400 kg, it accommodates one operator and four individuals weighing 80 kg each. Combined, these yield a total operating weight of 787 kg. This value remains within allowable thresholds for the frame, shock absorption, and braking mechanisms. Weight allocation across axles is labelled in Table 3.

Table 3. Component mass distribution.

Component	Mass (kg)
Chassis frame	114
Suspension/wheels	30
Motor and drivetrain	30
Battery pack (48 V, 100 Ah lead-acid)	136
Braking system	15
Electrical/wiring	10
Seats and interior	30

 doi:10.20944/preprints202603.1246.v1

Body panels (fiber-reinforced plastic)	22
Curb mass (vehicle only)	387
Payload (1 driver + 4 passengers)	400
Gross vehicle weight (GVW)	787

3. Methodology

The design followed a systematic multidisciplinary approach illustrated in Figure 1, progressing from requirements definition through simulation-based verification to final design.

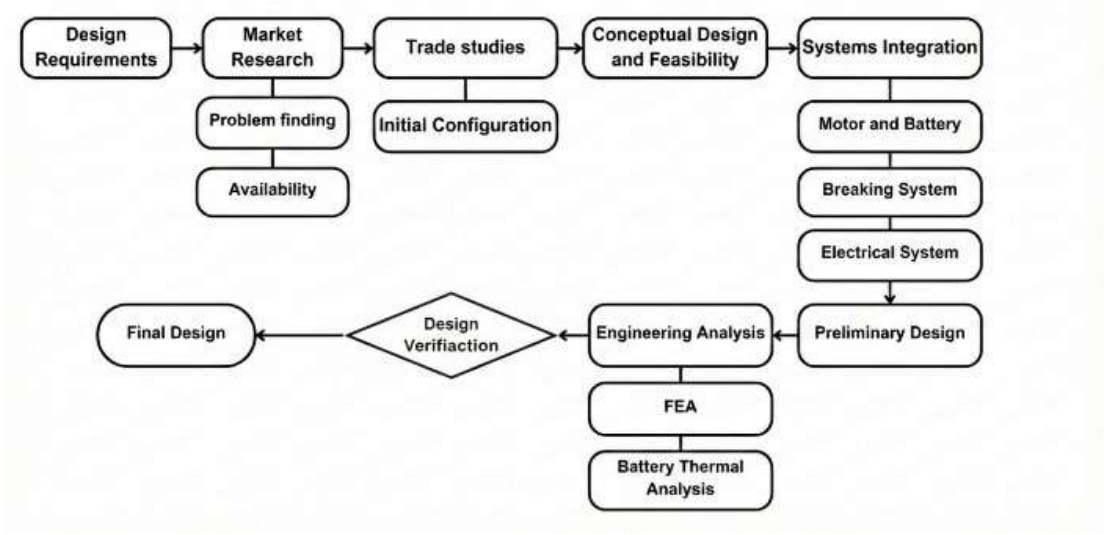

Figure 1. Design methodology flowchart.

3.1. Design Framework

Identified safety gaps in locally available electric three-wheelers guided the selection of design targets and materials. As rollover resistance was important, stability goals were based on Larson's test approach [21], aiming for at least 1,2 in static stability factor. The centre of gravity height was kept below 1 metre to support balance during motion. From 25 km/h, stopping within 10 metres became a firm benchmark, guided by FMVSS 135. Among the contenders, steel tubes are fused into a rigid frame structure. Power was provided by a 1200 W brushless motor mounted at the rear. Braking combined discs at the front with drums at the rear. Energy storage was positioned low beneath the occupants, aiding lower mass placement. Starting in SOLIDWORKS 2023, the concept layout shown in Figure 2 was developed through iterative modelling. Mass property calculations followed, providing early predictions of the centre of gravity and weight distribution across the frame. Components were designed as an integrated system. The motor and battery were positioned jointly, accounting for both space constraints and heat dissipation requirements. Stopping performance relied on a 330 mm rotor at the front paired with 130 mm drum units at the rear, both hydraulically actuated. Electrical functions included monitoring battery status and ensuring safe operation, including gas release provisions specific to lead-acid cells.

 doi:10.20944/preprints202603.1246.v1

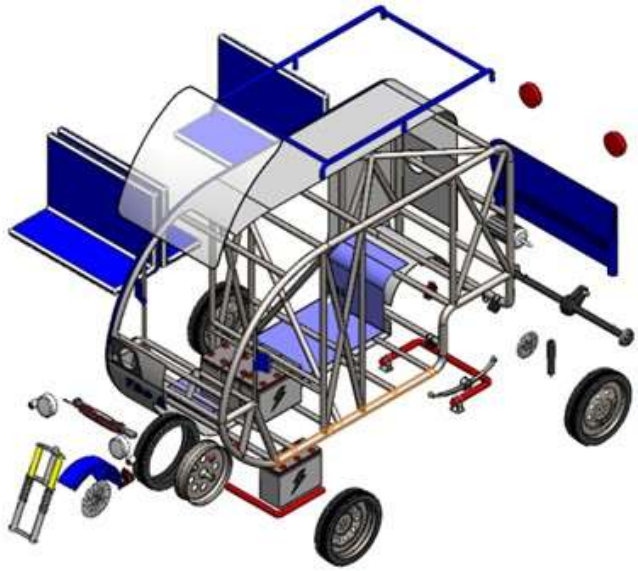

Figure 2. CAD Concept of the Three-Wheeler.

3.2. Structural FEA

Structural analysis using the finite element method was conducted in ANSYS Mechanical 2023 R1 for both the original easy-bike frame and the new tubular space-frame concept under two main loading scenarios. The front structural member was subjected to a constant force of 2080 N, with restraints applied to the rear supports. In the frontal impact simulation, the frame was subjected to an impact against a fixed rigid barrier at a velocity of 6,94 m/s (equivalent to 30 km/h) over 200 milliseconds. Time advanced automatically through explicit integration steps during this event. All attachment points along the rear axle remained fixed throughout each scenario. The material was defined as ST37 structural steel with density ρ = 7,85 g/cm³, Young's modulus E = 210 GPa, Poisson's ratio ν = 0,3, and yield strength 250 MPa. The element type used was SOLID185, a 3D solid, with a quadrilateral-dominant mesh for the impact analysis. The global element size was set to 20 mm, with local refinement to 10 mm in the impact zone, and gravitational acceleration of 9,81 m/s² applied in the vertical direction. Two chassis iterations were compared including the baseline design with 4985 elements and 8650 nodes achieving a Jacobian value of 0,82 and the new tubular space-frame consisting of 8792 elements and 15 006 nodes with a Jacobian value of 0,85.

3.3. Center of Gravity (CoG) Analysis

Starting with SolidWorks CAD models loaded to a total mass of 400 kg representing one driver and four occupants, the resulting centre of gravity is found at a vertical position of z = 0,642 m when weighted. The longitudinal centre of gravity lies slightly behind the midpoint along the x-axis, measured at approximately 1,586 m, which benefits rear-driven wheels during motion. Along the y-axis, lateral balance is closely aligned with the vehicle's central axis, showing minimal deviation. The static stability factor (Eq. 1) is calculated as half the distance between the tyres divided by the height of the centre of gravity, following the method described by Larson et al. [21]. This approach reflects standard practice in assessing rollover likelihood through physical proportions.

$$SSF = \frac{Track\ Width}{2 \times CoG\ Height} = \frac{1400}{2 \times 642,4} = 1,09 \quad (1)$$

Where track width is 1400 mm (rear wheel spacing) and CoG height is 0,642 m with full payload. Maximum lateral acceleration before rollover:

$$a_{max} = g \times SSF = 9,81 \times 1,09 = 10,7\ \text{m/s}^2 \quad (2)$$

Safe turning speed for a lane-change maneuver with turn radius 3,0 m:

 doi:10.20944/preprints202603.1246.v1

$$v_{safe} = \sqrt{a_{max} \times R} = \sqrt{10,07 \times 3} = 5,66 \text{ m/s} \quad (3)$$

3.4. Braking System Analysis

Braking force requirements were calculated for a 787 kg vehicle decelerating from 25 km/h to rest within 10 m (a = 2,41 m/s², 0,246 g). Total braking force required:

$$F_{brake,total} = m \times a = 787 \times 2,41 = 1895 \text{ N} \quad (4)$$

Force distribution was set at 60% front and 40% rear to account for weight transfer during deceleration, with 1137 N assigned to the front brakes to reflect dynamic load transfer and 758 N to the rear brakes to ensure residual stability and prevent wheel lock-up. Disc brake specifications included 330 mm diameter rotors, a friction coefficient μ ranging from 0,35 to 0,40 under wet conditions, and a pad contact area of 1500 mm².

3.5. Brake Thermal Analysis

Kinetic energy dissipated per stop from 25 km/h:

$$E_{kinetic} = \frac{1}{2} \times m \times v^2 = 0,5 \times 787 \times 6,94^2 = 18,95 \text{ kJ} \quad (5)$$

Assuming 60% front brake duty (E = 11,37 kJ per stop), and two 330 mm steel rotors (2 kg each, c_p = 500 J/kgK):

$$\Delta T_{per\ stop} = \frac{E}{\left(2 \times m_{rotor} \times c_p\right)} = \frac{11,370}{2 \times 2 \times 500} = 5,69 \text{ °C} \quad (6)$$

Over 10 consecutive emergency stops, assuming adiabatic conditions (no inter-stop cooling) as a conservative worst-case estimate:

$$T_{final} = T_{ambient} + \Delta T \times n = 35 + 5,69 \times 10 \approx 91,9 \text{ °C} \quad (7)$$

This conservative estimate remains well below the 200 °C brake fade threshold [19], confirming adequate thermal capacity with a margin of approximately 108 °C. In practice, convective cooling of the spinning rotors between stops would further reduce this temperature. Wet condition analysis indicates that in monsoon or post-rain operating conditions, the tyre–road friction coefficient decreases from μ = 0,38 under dry conditions to μ = 0,32 in wet conditions. Under maximum grip-limited braking, the stopping distance increases from 6,5 m to 7,7 m:

$$s_{wet} = \frac{v^2}{2 \times \mu_{wet} \times g} = \frac{6,94^2}{2 \times 0,32 \times 9,81} = 7,68 \text{ m} \quad (8)$$

This represents an increase of 18,8% compared to dry conditions, but remains well within the 10 m design target. The safety margin between required deceleration (0,246 g) and available tyre grip decreases from 35% (dry) to 23% (wet). Since kinetic energy per stop remains unchanged at 18,95 kJ regardless of surface conditions, rotor temperature rise is unaffected by wet operating conditions.

3.6. Motor Thermal Estimation

Motor thermal behaviour was estimated analytically for the 48 V, 1200 W BLDC motor under a one-hour urban duty cycle (30 min cruising at 60% load, 20 min stop-and-go at 40% load, 10 min idle). Motor efficiency is 88%, resulting in heat dissipation of 144 W at rated load. Under the 60% cruising load condition, heat dissipation is approximately 86–98 W. The average heat output over the full duty cycle is 90 W. Mounted under the seat with natural convection cooling (housing area A = 0,15 m², convection coefficient h = 5 W/m²K):

$$\Delta T_{motor} = \frac{Q_{loss}}{h \times A} = \frac{90}{5 \times 0,15} = 120 \text{ °C} \quad (9)$$

At 35 °C ambient, T_{motor} = 155 °C, approaching the BLDC insulation safety limit of 155 °C but acceptable for short-term operation. Addition of ventilation grilles or heatsink fins improves the convection coefficient. With partially obstructed airflow typical of the under-seat mounting position

 doi:10.20944/preprints202603.1246.v1

(h = 10 W/m²K), the estimated motor temperature decreases to 95 °C. Under fully effective forced convection conditions (h = 12 W/m²K), the temperature further decreases to 85 °C.

3.7. Electrical Safety Design

Rated at 48 V and 100 Ah, the lead-acid battery pack weighs 136 kg. Enclosed in aluminium alloy Al-6061, its structure relies on fully welded joints for integrity. Designed during initial planning, safety measures provide a triple margin against both steady forces and sudden impacts. Protection from vibration is provided by internal rubber dampers, calibrated to 60 Shore A firmness. Fluids exit through a dedicated 10 mm PVC conduit running beyond the chassis boundary. To prevent pooling, 5 mm openings help shed trapped moisture. With sealed edges throughout, leakage risks remain minimal under normal operation. Air moves through openings at the top and base, 15 holes, three millimetres wide, totalling about 50 mm² of space for air on every side, allowing hydrogen gas to escape during charging and high-load operating conditions, preventing pressure build-up. Power separation is achieved by a primary switch rated for 200 A, designed with springs that force it open if electricity stops flowing or if there is sudden movement, reacting in less than 100 ms. This component sits behind a safety link rated for 150 A, set to break at 165 A when heat rises too quickly, giving way in under 0,5 s. Wires carrying high currents run inside protective tubes, clearly marked by colour. Bright red indicates 48 V supply, black denotes the ground conductor. The path supplying energy to the drive unit includes a braking sensor operating across two circuits, cutting flow whenever braking begins at either wheel rim or front lever release (Figure 3).

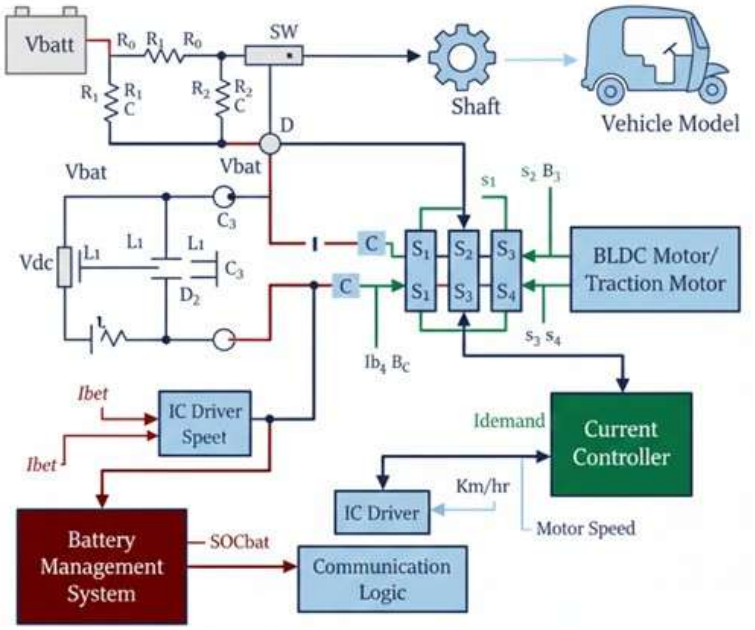

Figure 3. Electrical Circuit.

4. Structural FEA Results

4.1. Static Comparison

Deformation spreads across several components due to revised load paths and additional diagonal supports. At the front impact location, stress concentrates most intensely. The baseline frame exhibits a peak displacement of 1,059 mm at the front load application point (Table 4), while the redesigned chassis reduces this to 0,367 mm under identical conditions. The tubular space-frame (Figure 4) achieves this through additional diagonal bracing and optimised load paths, distributing deformation across multiple structural members rather than concentrating it at the front node, as observed in the baseline design (Figure 4).

 doi:10.20944/preprints202603.1246.v1

Table 4. Static deflection (2080 N front load, fixed rear support).

Parameter	Baseline frame / mm	Tubular space-frame / mm	Improvement
Max. deflection	1,059	0,367	65,4% reduction
Min. deflection	0,118	0,041	65,3% reduction
Deflection range	0,941	0,326	65,4% reduction

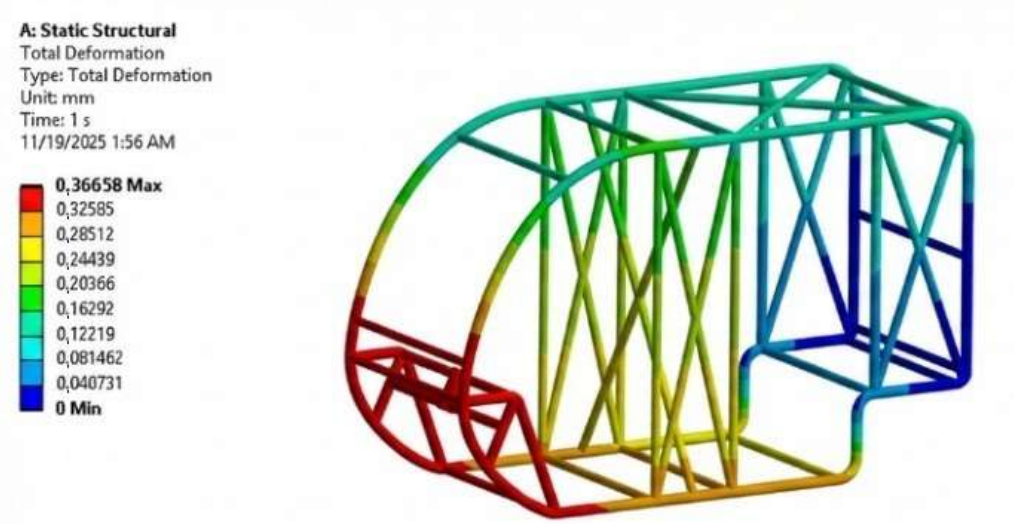

Figure 4. Tubular space-frame FEA.

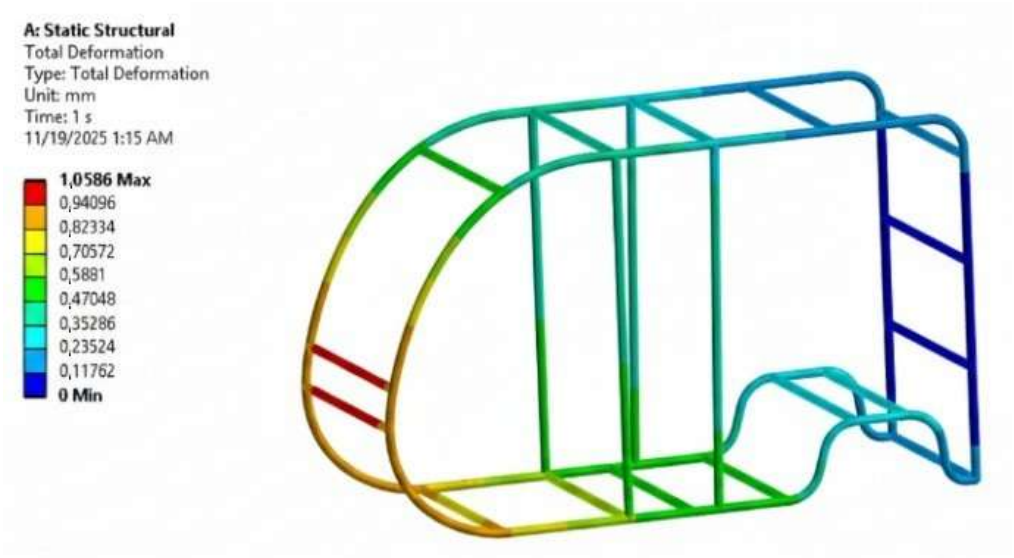

Figure 5. FEA Baseline design.

4.2. Dynamic Comparison

For the baseline frame (Figure 6), the maximum positive *z*-direction deflection is 76,5 mm, while the maximum negative deflection is −174,74 mm. The deformation is mainly concentrated in the upper front tubing and the diagonal members.

 doi:10.20944/preprints202603.1246.v1

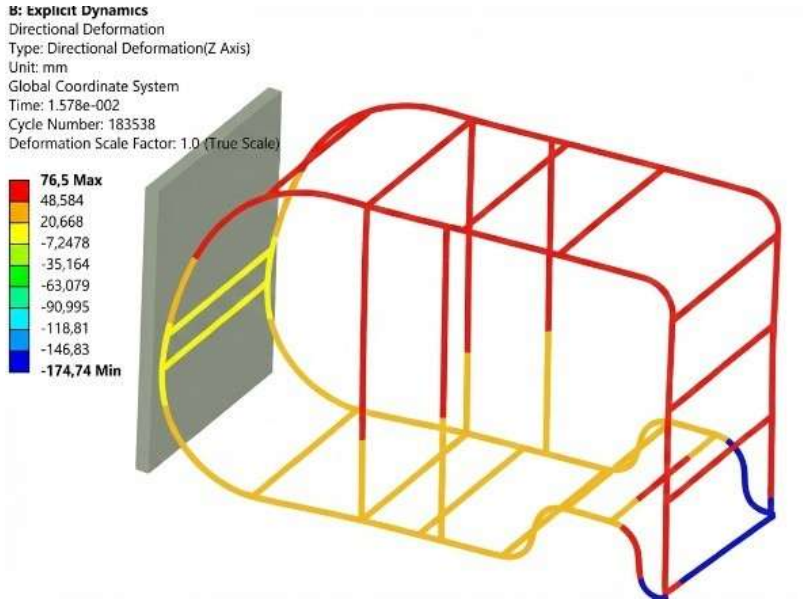

Figure 6. Baseline frame upon impact.

For the new tubular design (Figure 7), the maximum positive *z*-direction deflection is 64,604 mm, while the maximum negative deflection is −240,1 mm. The deformation is distributed across a denser bracing structure, resulting in higher and more uniform energy absorption.

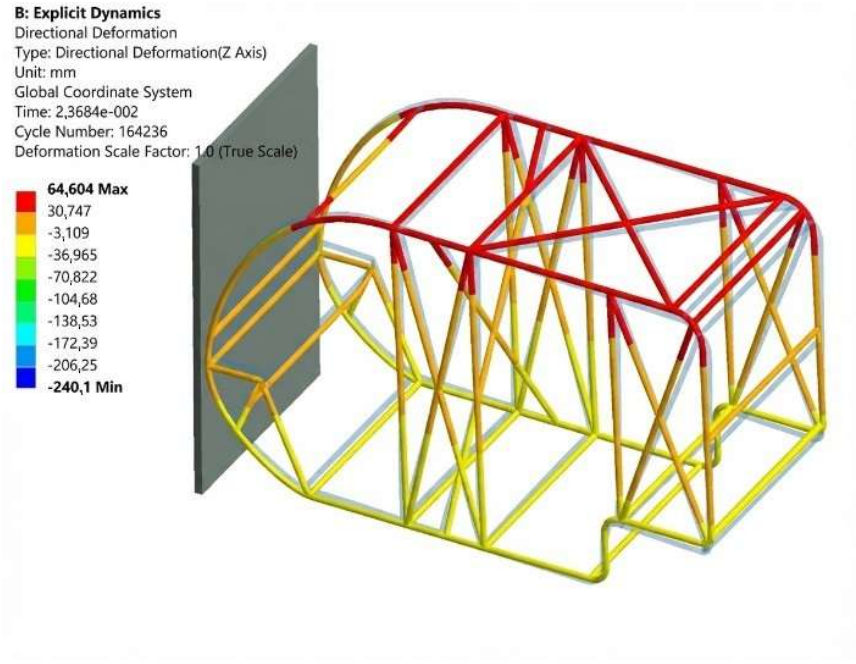

Figure 7. Tubular space-frame upon impact.

The new design absorbs impact energy more effectively through distributed deformation and multiple load paths, reducing localized stress peaks and improving occupant survivability in frontal collision scenarios (Table 5).

 doi:10.20944/preprints202603.1246.v1

Table 5. Frontal impact (6,94 m/s = 30 km/h).

Parameter	Baseline frame / mm	Tubular space-frame / mm	Improvement
Max positive z-deflection	76,5	64,6	15,6% reduction (stiffer)
Max negative z-deflection	−174,7	−240,1	37,3% higher (better absorption)
Deflection range	251,2	304,7	Distributed over more paths
Peak stress concentration	High (localized)	Lower (distributed)	Better spread
Mesh quality (Jacobian)	> 0,82	> 0,85	Improved convergence

5. Comparative Benchmarking

Performance gains in critical safety areas are evident when comparing the new model to those commonly used in Dhaka. The centre of mass is lowered by 10 %, at 0,642 m instead of 0,713 m [22], and plays a central role. As a result of this shift, static stability increases sharply by 35%, with the static stability factor rising from 0,809 (reported by Ekuase et al. [22] for a cargo-type tricycle of different configuration) to 1,09. This improvement is made possible by a 136 kg lead-acid battery mounted deep within the frame. Unlike older versions that position the battery behind the back axle, this version places it close to the ground. Braking performance shows the most significant improvement. Instead of relying solely on drums, the updated setup pairs large front discs (330 mm) with smaller rear drums (130 mm). The brake fade temperature margin exceeds 108 °C under worst-case repeated emergency braking conditions, confirming substantial thermal reserve.

Under steady force, the frame bends down to 0,37 mm compared to the earlier 1,0 mm when pressed with 2080 N at the front. This increased resistance indicates a stronger overall structure, supported by a hollow framework design that distributes forces through several channels. In head-on collision tests conducted at 30 km/h, deformation decreased noticeably and maximum positive deflection decreased by 15,6% (improved stiffness), while energy absorption increased by 37,3% due to greater distributed deformation across the tubular structure.

The cost premium is approximately 40% (1200–1400 EUR vs. 850–1050 EUR for baseline designs). This is driven mainly by the battery enclosure (~80 EUR), hydraulic disc brakes (~50 EUR vs. mechanical drums), and electrical safety hardware (~30 EUR). While higher than informal-sector easy bikes, the target cost remains within reach of commercial fleet operators (ride-hailing services, shared taxi networks), for whom improved safety reduces liability and maintenance costs.

Manufacturing feasibility remains high. All components and processes – mild steel welding, BLDC motor assembly, hydraulic brake installation – are available in Dhaka's existing rickshaw workshop infrastructure. The estimated labour requirement is 120–160 man-hours per unit, consistent with small-scale manufacturing (10–50 units/month) or pilot fleet production.

6. Discussion

The design achieves safety gains through passive geometric and material selection rather than active control systems. At 0,642 m, the centre of gravity yields a static stability factor of 1,09, which falls below the design target of 1,2 established in Table 2 and the benchmark of 1,2–1,3 recommended by Ataei et al. [5] To achieve SSF ≥ 1,2, the rear track width would need to increase to at least 1541 mm (from the current 1400 mm), or the CoG height would need to decrease to 583 mm. A combined approach—for example, widening the track to 1500 mm and reducing the CoG to 625 mm (SSF = 1,20)—may offer a practical compromise between stability and urban manoeuvrability in subsequent design iterations. Research by Rodríguez-Licea et al. [6] examined how three-wheeled vehicles in delta configuration tip when externally triggered, showing that dynamic stability aids are effective if brakes engage during the event. Rather than electronic intervention, this version relies on a lowered

 doi:10.20944/preprints202603.1246.v1

mass position combined with wider wheel spacing, favouring straightforward engineering over complex maintenance. Despite a design speed of 30 km/h, lateral forces remain within acceptable limits. The threshold reaches only 10,7 m/s² even during tight urban turns such as R = 3 m paths taken at 20,4 km/h without risk. Under repeated adiabatic braking (conservative worst-case), rotor temperature peaks at 92 °C after 10 consecutive emergency stops. This remains well below critical levels, maintaining a margin of 108 °C below the 200 °C fade threshold. Earlier work by Jaenudin et al. [12], using finite element methods, recorded higher values between 220 °C and 250 °C after just five decelerations. Cooler operation here results partly from reduced energy per stop, only 18,95 kJ, combined with improved mass distribution across brake components, reflecting a lighter overall weight compared to standard automobiles. While earlier versions struggled with loose wiring, gas buildup, or impact risks, the Al-6061 housing now incorporates a threefold safety buffer against such hazards. Design validation relies on digital tools such as CAD-derived weights, structural simulations, and mathematical heat flow predictions without depending on laboratory experiments. Though useful, the simulation assumes materials respond uniformly under load, omitting permanent deformation or failure modes such as wrinkling seams or broken joints. Zamzam et al. [8] modelled an electric vehicle chassis during a 30 km/h speed bump event using transient finite element analysis, finding maximum stress reached 289 MPa. For brake heating evaluation, researchers applied fixed surroundings at 35°C along with uniform rotor temperatures, disregarding internal variations and time-dependent dissipation. Heat behaviour in the motor assumes steady flow patterns and here the upper threshold of 155°C matches NEMA Class F standards [20]. The present work constitutes a numerical design study. All structural, thermal, and stability results are based on computational models and analytical calculations. To verify real-world performance, tests such as crash simulations, brake measurements, heat scans, and live trials must be conducted before manufacturing.

Each component was selected to suit Dhaka's informal production environment. The ST37 tubular chassis is fabricated using GMAW welding, a technique standard in Dhaka's rickshaw repair workshops. The 48 V lead-acid batteries, available throughout the city's e-rickshaw networks, power the 1200 W BLDC motor. Motorcycle parts suppliers provide the 330 mm hydraulic disc brakes. Fabrication of Al-6061 enclosures depends on access to TIG welding, a service available in standard industrial workshops. While materials pose little difficulty, maintaining consistent weld quality remains the main challenge. To address this, defined welding procedures are used, along with controlled torque application for electrical joints and established methods for brake system fluid evacuation. Training lasting two or three days generally supports these practices effectively. Estimates of cost versus performance rely on assumptions linked to design changes measured here; actual results may vary until confirmed by real-world operation records. A price difference of 40 % ranging from 1200 to 1400 EUR compared to 850 to 1050 EUR for standard models is justified by reduced costs associated with collisions. Maintenance intervals are extended in real-world use, particularly at the rear axle, where friction components last longer. Vehicle uptime improves significantly. Currently, no official regulations govern e-rickshaw safety at the national level in Bangladesh. What has been introduced provides foundational criteria that could inform future BNS policy development. Early adoption on a non-mandatory basis enables practical performance data collection before any regulatory action.

Despite progress, BSTI may introduce a metric-driven benchmark including static stability factor (SSF), stopping ability, frame resilience, and electrical protection. At a later stage, adherence could shift towards compulsory validation through model certification paired with oversight checks. Future work should address integration with charging infrastructure and electromagnetic compatibility. Bidirectional AC-DC converters for fast charging and standardised EMC testing protocols are relevant considerations for commercial deployment of electric three-wheelers in dense urban environments [23,24].

 doi:10.20944/preprints202603.1246.v1

Funding: This research paper was funded by the University of Slavonski Brod through the institutional research project Analysis of the influence of design and process parameters of FDM technology on the mechanical and vibrational properties of polyamide PA6 tooth of a cylindrical spur gear for the purpose of optimizing the hybrid infill structure design (ASPFDM-PA6), financed by the European Union – NextGenerationEU. The views and opinions expressed in this paper are those of the author and do not necessarily reflect the official position of the European Union or the European Commission. Neither the European Union nor the European Commission can be held responsible for them.

Conflicts of Interest: The authors declare no conflict of interest.

References

1. Hambissa, D., Nallamothu, R. B., & Andarge, T. (2022). Analysis of Three-Wheeler Vehicle Structure at the Event of Side Pole Crash. *Journal of Engineering*, 5490585. https://doi.org/10.1155/2022/5490585
2. [Hossain, M. J. A., Hasan, M. Z., Hasanuzzaman, M., Khan, M. Z. R., & Ahsan Habib, M. (2023). Affordable Electric Three-Wheeler in Bangladesh: Prospects, Challenges, and Sustainable Solutions. Sustainability, 15(1), 149. https://doi.org/10.3390/su15010149
3. Nguyen, X.N. & Tran, T.T. (2023). Rollover stability dynamic analysis of passenger vehicle in moving conditions. *Mathematical Modelling of Engineering Problems*, *10*(1), 149-154. https://doi.org/10.18280/mmep.100116
4. Ketemaw, D. & Seid, S. (2022). Design of a rollover index-based sliding mode controller for roll stability of three wheeled vehicles using rear differential braking. *Front. Mech. Eng 8*, 1038289. https://doi.org/10.3389/fmech.2022.1038289
5. Ataei, M., Khajepour, A., & Jeon S. (2017). Rollover stabilities of three-wheeled vehicles including road configuration effects. *Proceedings of the Institution of Mechanical Engineers, Part D: Journal of Automobile Engineering*, *231*(7), 859-871. https://doi.org/10.1177/0954407017695007
6. Rodríguez-Licea, M.-A. (2021). On the Tripped Rollovers and Lateral Skid in Three-Wheeled Vehicles and Their Mitigation. *Vehicles*, *3*(3), 357-376. https://doi.org/10.3390/vehicles3030022
7. Jin, Z., Li, J., Huang, Y. et al. (2019). Study on Rollover Index and Stability for a Triaxle Bus. *Chin. J. Mech. Eng*, *32* (64) (2019). https://doi.org/10.1186/s10033-019-0376-0
8. Zamzam, O., Ramzy, A. A., Abdelaziz, M., Elnady, T., & El-Wahab, A. A. A. (2025). Structural performance evaluation of electric vehicle chassis under static and dynamic loads. Scientific reports, *15*(1), 5168. https://doi.org/10.1038/s41598-025-86924-w
9. Ayyakkannu, V., Sri Ram, P., & Vijayakumar, V. (2024). Analysis of the Roll Cage of an Electric All Terrain Vehicle (e-ATV) Using the Finite Element Method, *SAE Technical Paper* 2023-01-5178. https://doi.org/10.4271/2023-01-5178
10. FMVSS 135. Federal Motor Vehicle Safety Standard - Light vehicle brake systems. Retrieved from https://unece.org/DAM/trans/doc/wp29compendium/6-3.pdf
11. Talati, F., & Jalalifar, S. (2009). Analysis of heat conduction in a disk brake system. *Heat Mass Transfer 45*, 1047–1059. https://doi.org/10.1007/s00231-009-0476-y
12. Jaenudin, Jamari, J., & Tauviqirrahman, M. (2017). Thermal analysis of disc brakes using finite element method. *AIP Conf. Proc., 1788* (1), 030028. https://doi.org/10.1063/1.4968281
13. Damodaran, V., Murugan, S., Shigarkanthi, V., Nagtilak, S. et al., (2011). Thermal Management of Lead Acid Battery (Pb-A) in Electric Vehicle, *SAE Technical Paper* 2011-01-0653. https://doi.org/10.4271/2011-01-0653
14. Yavuz, B., Arıcı, M. i Nižetić, S. (2023). A systematic review on battery thermal management systems for electric vehicles. *Engineering Power*, *18* (2-3), 27-40. Retrieved from https://hrcak.srce.hr/326799
15. Li, A., Ponchant, M., Sturm, J., & Jossen, A. (2020). Reduced-Order Electro-Thermal Battery Model Ready for Software-in-the-Loop and Hardware-in-the-Loop BMS Evaluation for an Electric Vehicle. *World Electric Vehicle Journal*, *11*(4), 75. https://doi.org/10.3390/wevj11040075

 doi:10.20944/preprints202603.1246.v1

16. Nguyen, D. N., Nguyen, T. A., & Dang, N. D. (2022). A complex rollover dynamics model with active stabilizer bar controlled by the fuzzy algorithm. *Heliyon*, *8*(11), e11715. https://doi.org/10.1016/j.heliyon.2022.e11715
17. Chen, J., Wang, R., Liu, W., Sun, D., Jiang, Y., & Ding, R. (2025). A Review of Recent Advances in Roll Stability Control in On-Road and Off-Road Vehicles. *Applied Sciences*, *15*(10), 5491. https://doi.org/10.3390/app15105491
18. Du, J., Sun, Y., Zhao, J., Liu, B., & Mi, Y. (2025). Loss Research and Thermal Analysis of BLDC Hollow-Cup Motor Under Reactor Suppression. *Applied Sciences*, *15*(3), 1523. https://doi.org/10.3390/app15031523
19. Bellini, C., Di Cocco, V., Iacoviello, D., & Iacoviello, F. (2024). Temperature Influence on Brake Pad Friction Coefficient Modelisation. *Materials*, *17*(1), 189. https://doi.org/10.3390/ma17010189
20. NEMA MG 1-2021. Motors and Generators Standard.
21. Larson, R., Smith, J., Werner, S., and Fowler, G. (2000). Vehicle Rollover Testing, Methodologies in Recreating Rollover Collisions, SAE Technical Paper, 2000-01-1641. https://doi.org/10.4271/2000-01-1641.
22. Ekuase, A. , Aduloju, S. C, Ogenekaro, P., O., Ebhota, W. S. & Dania, D. E. (2015). Determination of Center of Gravity and Dynamic Stability Evaluation of a Cargo-type Tricycle. *American Journal of Mechanical Engineering*, *3*(1), 26-31. https://doi.org/10.12691/ajme-3-1-5
23. Abras, J. i Vural, A.M. (2025). Design of 100 kW Three-Phase Bidirectional AC-DC Matrix Converter for Fast Charging of Electric Vehicles. *Tehnički vjesnik*, *32* (2), 407-414. https://doi.org/10.17559/TV-20240527001680
24. Güler, S. (2026). Electric Vehicle Electromagnetic Compatibility Testing and Electromagnetic Emission Mitigations. *Tehnički vjesnik*, *33*(1), 315-323. https://doi.org/10.17559/TV-20241022002085